Influence of Type and Content of Various Comonomers on Long-Chain Branching of Ethene/α-Olefin Copolymers

Florian J. Stadler,[†] Christian Piel,[§] Katja Klimke,[‡] Joachim Kaschta,[†] Matthew Parkinson,[‡] Manfred Wilhelm,[‡,⊥] Walter Kaminsky,[§] and Helmut Münstedt*,[†]

Institute of Polymer Materials, Department of Materials Science, University Erlangen-Nürnberg, Martensstr. 7, D-91058 Erlangen, Germany; Max Planck Institute for Polymer Research, Ackermannweg 10, D-55128 Mainz, Germany; Institute of Technical and Macromolecular Chemistry, University Hamburg, Bundesstr. 45, D-20146 Hamburg, Germany; and Institute of Mechanics, Technical University Darmstadt, Hochschulstr. 1, D-64289 Darmstadt, Germany

Received June 29, 2005; Revised Manuscript Received November 29, 2005

ABSTRACT: One polyethylene and nine ethene/α-olefin copolymers differing in amount (0.4−2.9 mol %) and molar mass of the comonomer were characterized by NMR, SEC-MALLS, and rheology. Samples were polymerized using a $[Ph_2C(2,7\text{-di-}t\text{-BuFlu})(Cp)]ZrCl_2$/MAO catalyst, with octene, octadecene, and hexacosene as comonomers, resulting in polymers of $M_w \approx 190$ kg/mol. The comonomer content was determined by melt-state NMR. For the homopolymer 0.37 and 0.30 LCB/molecule were found by NMR and SEC-MALLS, respectively. Rheological quantities, such as the zero shear rate viscosity (η_0), increased with LCB as compared to linear samples of the same M_w. The shape of the viscosity function and the linear steady-state elastic compliance (J_e^0) showed a dependence on comonomer content and length. These findings are used to elucidate the various long-chain branching architectures. The highest comonomer content samples behaved like typical linear polymers in rheological experiments, while those with less comonomer contents were found to be long-chain branched. Besides the comonomer content, the type of comonomer has an influence on the branching structure.

Introduction

The synthesis and characterization of polyolefins, especially polyethylenes (PE) and ethene/α-olefin copolymers synthesized using metallocene catalysts, have gained great interest in recent years. This is due to several major advantages of these systems over those produced by Ziegler−Natta (Z−N) catalysis. With metallocene catalysis, the molar mass is adjustable over a broad range,[1] and the polymers show a narrow molar mass distribution (MMD).[2,3] Because of the stereo- and regiospecific nature of the catalysts, highly tactic and tailored copolymers may be produced.[4−6] Metallocene catalysts also have a high affinity to incorporate α-olefins into growing chains and are even able to produce homopolymers of these higher α-olefins.[7−9] In contrast, copolymerization of α-olefins with more than eight carbon atoms by Z−N catalysts proves difficult. Polymer chains containing a terminal vinyl group, created in situ, can also act as macrocomonomers, leading to the formation of long-chain branched (LCB) polymers.

Single-site catalysts produce a novel structure combination for LCB-PE with narrow molar mass distribution being first reported in patent literature in the mid-1990s.[10,11] The first scientific papers covering this topic were published a few years later.[12−14] Evidence for long-chain branching in metallocene PE (mPE) was published by Wood-Adams et al.[15] using a combination of NMR, SEC, and shear rheology. However, for the quantification of the small amount of LCB by NMR extremely long measurement times, of up to 2 million scans, were needed.

Most constrained geometry catalysts found to produce LCB are either half-metallocenes[10,16] or ansa-metallocenes.[17−19] The non-ansa-metallocene Cp_2ZrMe_2 system, activated with either $B(C_6F_4)_3$ or methylalumoxane (MAO), was also reported to produce long-chain branches.[1,11,12,19,20] Long-chain branching in metallocene-catalyzed polymerizations is believed to take place via a copolymerization route, with the incorporation of a vinyl-terminated polyethylene chain into a growing polymer chain.[12,21,22] Investigation into the polymerization behavior of several metallocene catalysts revealed that the termination mechanisms were catalyst specific. Depending on the catalyst structure, the termination of chain growth occurred via either β-H elimination, hydrogen transfer to the monomer, or chain transfer to the cocatalyst. Further research indicated that catalysts with high vinyl selectivity and good copolymerization ability were the most prominent for producing polymers with modified rheological properties.[23,24]

The formation of LCB depends on many different factors, including the presence of comonomers. If α,ω-dienes are incorporated, the additional terminal vinyl groups act as starting points for long-chain branching and thus result in a higher degree of LCB.[24] Initial investigations indicated that α-olefin comonomers decrease the amount of LCB, as they tend to terminate the growing chain.[25] The resulting vinylidene group at the end of a macromer is believed to be sterically hindered from reintroduction into a growing chain by the short-chain branch residing at the 2-position. Additionally, vinyl-terminated polymer chains are sterically hindered from incorporation as LCB due to the short-chain branches in the growing chain and macromonomer. Thus, the degree of LCB tends to decrease with increasing comonomer content.

It was shown by Kokko et al.,[19] for the catalyst system *rac*-$[Et(Ind)_2]ZrCl_2$/MAO, that both the temperature dependence of the viscosity and the viscosity (at an angular frequency of $\omega = 0.02\ s^{-1}$) itself decreased when introducing up to 3.4 mol % hexadecene. This finding was explained by a decreasing amount

[†] University Erlangen-Nürnberg.
[‡] Max Planck Institute for Polymer Research.
[§] University Hamburg.
[⊥] Technical University Darmstadt.
* Corresponding author: e-mail helmut.muenstedt@ww.uni-erlangen.de, Fax +49 9131 852 8321.

10.1021/ma0514018 CCC: $33.50
Published on Web 01/19/2006

of LCB. However, the data indicated that 3.4 mol % comonomer was not sufficient for the complete suppression of LCB. The viscosity at $\omega = 0.02\ s^{-1}$ was distinctly above the zero shear-rate viscosity of a linear polymer of equal molar mass; the activation energy of 41 kJ/mol was also much higher than that expected for a truly linear HDPE system (28 kJ/mol).[26] It was also shown that the presence of gaseous hydrogen during polymerization dramatically decreased the degree of long-chain branching using certain metallocene catalysts.[19,24] Investigation of the combined influence of hydrogen and α-olefins, although commonly used in industry to tailor PE properties, has to date not been undertaken.

Long-chain branches are known to strongly influence the processing behavior of PE by not only increasing the shear thinning behavior at smaller angular frequencies/shear rates but also improving the stability of elongation-dominated processes by strain hardening. Some aspects of the processing behavior can be assessed by measuring the viscosity function in shear and extension.[27]

The investigation of the influence of comonomer content and comonomer size on LCB using melt-state NMR, SEC-MALLS, and linear viscoelastic shear rheology is presented in this paper. The combination of these methods was found to be a very powerful method to characterize LCB in short-chain branched metallocene polyethylenes (LCB-mLLDPE), with various chemical composition. Although the influences of comonomer and hydrogen on LCB have previously been separately investigated, their combined interaction has not been studied. The data presented herein is thought to be the first comparison of LCB for different comonomers in the presence of hydrogen during polymerization. Furthermore, to our knowledge hexacosene is the longest narrowly distributed comonomer used for mPE so far. All polymers were synthesized using the same catalyst system under comparable conditions.

Characterizations of LCB in polyolefins produced with this particular catalyst by rheology, melt-state NMR, and SEC-MALLS have not previously been reported. Melt-state NMR was used to quantify the comonomer content in the copolymers and the degree of LCB in the homopolymer. Because of the lack of chemical shift resolution, LCB was defined as branches of ≥C4, as found elsewhere in the literature,[15] and thus represents an upper limit of possible long-chain branching. The influence of short-chain branching on crystallization and solid-state mechanical properties was also studied and is published elsewhere.[28]

Experimental Section

Synthesis. A set of 10 polymers was synthesized under similar conditions using the metallocene [Ph_2C(2,7-di-*t*-BuFlu)(Cp)]$ZrCl_2$[1] as catalyst precursor and methylalumoxane (MAO) as cocatalyst. Experimental details are described elsewhere.[23] The mPE samples differ only in length and amount of comonomer. As comonomer, the α-olefins octene, octadecene, and hexacosene (C_{26} containing C_{28} impurities) were used. For reference, an ethene homopolymer was synthesized under similar conditions.

A summary of the synthesized products and monomer feeds is given in Table 1. All reactions were carried out at 60 °C, with 9 mmol of hydrogen gas fed into the reactor prior to polymerization. (The homopolymer F0 is the same sample as F3 in a related publication.[1])

Molecular Characterization: Size Exclusion Chromatography/Multiangle Laser Light Scattering (SEC-MALLS). Molecular characterization was carried out by means of a high-temperature size exclusion chromatograph (Waters, 150C) equipped with refractive index (RI) and additional infrared (IR) (PolyChar, IR4) detectors. All measurements were performed at 140 °C using 1,2,4-trichlorobenzene (TCB) as solvent. The high-temperature SEC was coupled with a multiangle laser light scattering (MALLS) apparatus (Wyatt, DAWN EOS). Details of the experimental SEC-MALLS setup and conditions of use have previously been published.[29]

Table 1. Compositions of the Samples

sample	comonomer	feed [mol %][a]
F0	none	0
F8A	1-octene	10
F8B	1-octene	15
F8C	1-octene	20
F18A	1-octadecene	5
F18B	1-octadecene	15
F18C	1-octadecene	20
F26A	1-hexacosene	5
F26B	1-hexacosene	15
F26C	1-hexacosene	20

[a] Total monomer concentration was 0.5 mol/L for all copolymerizations and 0.41 mol/L for HDPE F0.

Nuclear Magnetic Resonance Spectroscopy. Melt-state NMR spectroscopy was carried out on a Bruker Advance 500 dedicated solid-state NMR spectrometer operating at a proton and carbon Larmor frequency of 500.13 and 125.75 MHz, respectively. All measurements were undertaken using a commercial Bruker $^{13}C-^{1}H$ optimized, high-temperature, 7 mm magic-angle spinning (MAS) probehead using zirconia rotors and rotor caps. Nitrogen gas was used for all pneumatics to limit thermal oxidation. All measurements were conducted at $\omega_r/2\pi = 3$ kHz spinning speed at 150 °C sample temperature, while compensating for thermal MAS effects.

Single-pulse excitation spectra were acquired using 10 μs ^{13}C $\pi/2$ excitation pulses and π pulse-train heteronuclear dipolar decoupling. For the copolymers, depending on degree of incorporation, between 16 and 424 scans were needed to achieve the desired signal-to-noise-ratio of the α peak at 34.6 ppm ($SNR_\alpha = 50$) using a 2 s recycle delay and 16 dummy scans. The overall measuring time of all copolymer samples was about 45 min. Short measurement times were primarily achieved due to investigation in the bulk state, combined with the use of a short recycle delay.[30] For the homopolymer (F0) 78 000 scans were acquired under the same conditions and resulted in a $SNR_\alpha \approx 5$ after 48 h.

Rheological Characterization. Rheological measurements were carried out on constant stress rheometers (Bohlin/Malvern CVOR "Gemini" and a Bohlin/Malvern CSM) using a 25 mm parallel plate geometry at 150 °C. To prevent thermal degradation during measurement, all samples were stabilized with 0.5 wt % Irganox 1010 and Irgafos 168 (CIBA SC, Basel), and the oven of the rheometers was purged with nitrogen.

Frequency sweeps, in the linear viscoelastic regime, were performed in the angular frequency range between 0.01 and 1000 s^{-1} using the stress-controlled mode. With the frequencies applicable in the dynamic-mechanical tests not low enough to reach the terminal regime for both viscosity $|\eta^*(\omega)|$ and the storage compliance $J'(\omega)$ all samples were also characterized by creep and creep recovery at stresses providing linear viscoelastic response. A detailed description of the experimental method used for the creep and creep recovery experiments can be found elsewhere.[31]

The creep compliance $J(t')$ is the deformation normalized by the constant stress τ applied. The creep recovery compliance $J_R(t)$ is the elastic part of the creep deformation normalized by the constant stress τ. It is measured by the reversible deformation of the sample after the stress ceases.

Two examples of creep and creep recovery tests are shown in Figure 1. The sample F8A had the higher zero shear rate viscosity $\eta_0 = 1.22 \times 10^6$ Pa s in comparison to F26C, with $\eta_0 = 0.087 \times 10^6$ Pa s. The creep recovery compliance $J_R(t)$ of F8A was a factor of 10 higher than that of F26C. The creep stress τ for both samples was chosen within the linear viscoelastic regime.

The long measurement times necessary to obtain the steady state of $J(t')$ and $J_R(t)$ illustrate the need for thermal stability. To check for thermal degradation, frequency sweeps before and after the creep and creep recovery tests were compared. A deviation of $G'(\omega)$ by

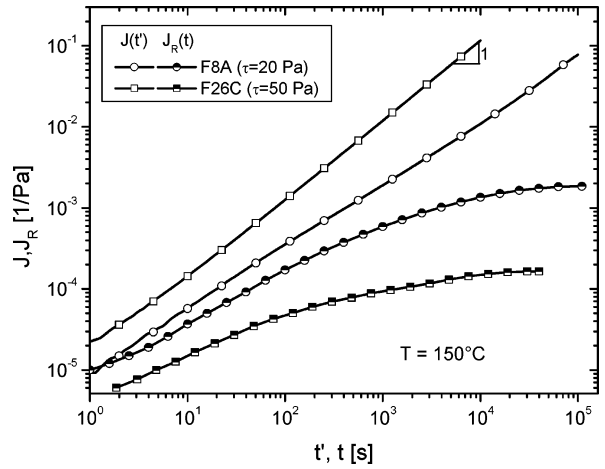

Figure 1. Creep and creep recovery compliance of F8A and F26C.

no more than ±5% was taken as the stability criterion. All products were found to be stable for at least 20 h at 150 °C, with some stable for more than 70 h.

The creep recovery compliance $J_R(t)$ data were transformed into $G'(\omega)$ and $G''(\omega)$ (this is only possible if the terminal regime is reached in the creep test and if the creep stress τ is low enough that the test is conducted in the linear viscoelastic regime) by determining a discrete retardation spectrum according to the method of Kaschta and Schwarzl.[32] It was thus possible to obtain the storage and loss modulus in a frequency range of at least 7 decades without performing any kind of time−temperature superposition (TTS). This was of particular importance as LCB polyethylenes are not thermorheologically simple fluids.[33] Furthermore, the low activation energy in combination with a small experimental temperature window ($T_m < T < T_{degradation}$) reduces the benefit of TTS.

Results and Discussion

Molecular Characterization: NMR. An estimation of comonomer incorporation was achieved by integration of the signals of the quantitative proton-decoupled ^{13}C melt-state NMR (cf. Figure 2). The ratio of integrals associated with a branch site to that of the bulk backbone CH_2 sites (A_{bulk}) allows direct access to the degree of incorporation. Although the actual CH branch site (*) is resolved at 38.3 ppm, the three sites adjacent to this (α) at 34.6 ppm are used for branch quantification due to their increased sensitivity. The comonomer incorporation, in units of mol % (n_c) and wt % (w_c), was calculated from the relative area of the α peak at 34.6 ppm (A_α) to that of the bulk peak at 30 ppm (A_{bulk}) using

$$n_c = 100 \times 2 \times \frac{\frac{1}{3}A_\alpha}{A_{bulk} + \frac{1}{3}A_\alpha(4 - n_\delta - n_4)} \text{ [mol \%]} \quad (1)$$

$$w_c = \frac{n_c l}{n_c(l-2)+2} \text{ [wt \%]} \quad (2)$$

where n_δ and n_4 are the number of δ and 4 sites per branch and l is the total number of carbons in the comonomer. The factors of 2 and $^1/_3$ in eq 1 combine the influence of the two backbone carbon sites per mole of monomer and the three α sites per branch. The term $^1/_3A_\alpha(4 - n_\delta - n_4)$ corrects A_{bulk} so that only the backbone sites are represented by the denominator.

It should be noted that in the melt state the δ, γ, and 4-sites are integrated as a single peak A_{bulk}. A number of assumptions are made when using the area of this peak as an internal standard representing the backbone. Because of the broad base of the peak at 30 ppm in the melt state, the integral range is limited by neighboring peaks at 32.2 and 37.2 ppm. This leads to an underestimation of A_{bulk} and correspondingly to an overestimation of the branching. However, when considering the relative sizes of the areas in question (see Figure 2), the differences between the true and approximated values of A_{bulk} are small and propagate into only minor deviations in calculated comonomer incorporation.

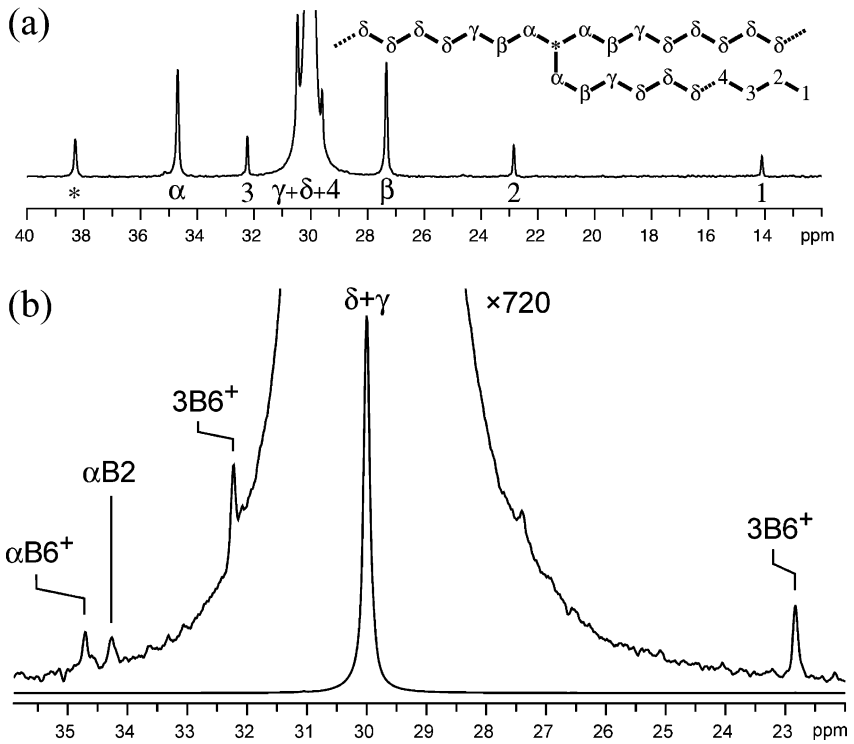

Figure 2. (a) Typical melt-state ^{13}C NMR SPE spectrum and assignment of polyethylene containing branches of six carbons in length or longer (F18C: 13.7 branches per 1000 backbone carbons). (b) Melt-state spectrum of the homopolymer showing 8 ethyl and 6 hexyl or longer branches per 100 000 CH_2 (F0: 78 000 scans).

Table 2. Results of Analytical and Rheological Characterizations of PE and Copolymer Samples

sample	comonomer [C_nH_{2n}]	comonomer feed [mol %]	n_c [mol %][a]	w_c [wt %][a]	M_w [kg/mol]	M_n [kg/mol]	M_w/M_n	η_0 [kPa s][b]	J_e^0 [10^{-4} Pa^{-1}]
F0		0	0.012 (<C2)/ 0.016 (>C2)[c]		173	85	2.0	445	12
F8A	8	10	1.1	4.3	240	112	2.1	1224	18[d]
F8B	8	15	1.8	6.8	190	92	2.0	440	11
F8C	8	20	2.7	10.0	152	76	2.0	51	2.2
F18A	18	5	0.4	3.5	183	80	2.3	498	15
F18B	18	15	1.5	12.1	167	84	1.9	164	6.4[d]
F18C	18	20	2.2	16.8	159	79	1.9	55	1.4
F26A	26	5	0.5	6.1	185	89	2.1	450	11
F26B	26	15	1.6	17.4	194	82	2.1	284	7.6[d]
F26C	26	20	2.3	23.4	175	78	2.1	87	1.6

[a] As determined by melt-state NMR. [b] At 150 °C. [c] Branches >C_2 are taken to be the upper limit of the long-chain branch content (0.37 LCB/molecule). [d] Steady-state of elastic recovery compliance J_e^0 not proven to be reached.

As well as the error in incorporation calculation, another source of error lies in the shorter than usual recycle delay τ_{rd} of 2 s used to acquire the spectra. This is less than the common criteria of $\tau_{rd} > 5T_1^C$ for quantitative NMR, where $T_1^\alpha \approx 0.5$ s and $T_1^{bulk} \approx 1.5$ s. However, it has previously been shown that under these conditions branch quantification using A_α and A_{bulk} is still valid.[30]

Considering these sources of error, the comonomer incorporations as determined by melt-state NMR are given to one decimal place. Repeating the branch quantification for a low (F26A) and high (F18C) incorporation sample 20 times gave a relative standard deviation in branch content of 2.0 and 2.9%, respectively.

For the homopolymer F0 the higher number of scans (78 000) allowed for the determination of lower branch contents. Because of the broad nature of the "foot" of the bulk peak, all CH_2 sites are incorporated into A_{bulk}, including the α branch sites. Separate integration of the branch sites only (A_{br}) allows the branch content (B_{br}) per CH_2 to be calculated from the ratio $B_{br} = A_{br}/A_{bulk}$. It should be noted that for ethyl branches $A_{br} = {}^1/_2A_\alpha$ whereas for hexyl and longer branches $A_{br} = {}^1/_3A_\alpha$.

Under these conditions ~0.03 mol % branching was still seen. Such branches may occur in metallocene-catalyzed homopolymerizations via isomerization reactions, although these are less important for polyethylenes than for polypropylenes. The degree of branching was found to be approximately evenly distributed between ethyl and hexyl or longer branches, corresponding to 0.8/10 000 CH_2 and 0.6/10 000 CH_2, respectively. Thus, the average molecule of F0 had ~0.37 branches of 6 or more carbons. With no comonomer used, this number was taken as an upper limit of the possible amount of LCB present. It should be stated that the absolute number of LCB cannot be determined by melt-state NMR as no chemical shift distinction is seen between branches of 6 carbons in length and those of the entanglement molar mass M_e (≈100C, see Stadler et al.[29] for a detailed analysis of the literature data). However, only branches greater than M_e are considered long-chain branches relevant for processing.

It is evident that only a fraction of the feed (≈10%) is incorporated into the polymer (Table 2). Although the maximum comonomer content (n_c) of F26C seems small, the comonomer accounts for about 20 wt % of the sample, due to hexacosene having ~13 times molecular weight than ethene. For the F8 and F18 copolymers the amount of comonomer does not play such a decisive role concerning weight fraction.

SEC-MALLS. The distributions of molar mass of the three polyethylene cooctenes F8 are shown in Figure 3. The molar mass distribution of all polymers investigated shows a narrow distribution $M_w/M_n \sim 2$, typical of metallocene catalysis. The products differed in molar mass averages M_w only, with none showing a high molecular weight component.

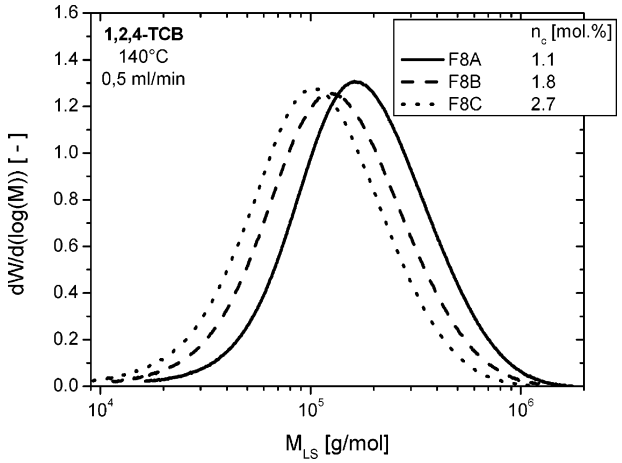

Figure 3. Molar mass distribution of the polymers of the octene series.

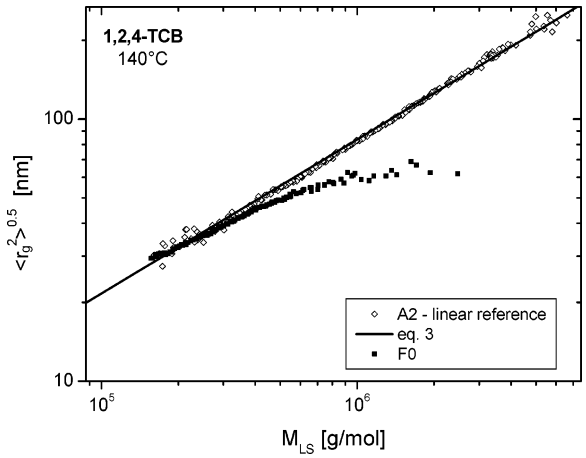

Figure 4. Radius of gyration as a function of absolute molar mass for a linear reference polymer (A2) and the homopolymer (F0).

When the radius of gyration of F0 was compared to a known linear reference A2, evidence for LCB was found (Figure 4). Detailed information on the linear reference is given elsewhere.[29] The straight line for the linear sample in Figure 4 can be described by

$$\langle r_g^2 \rangle^{0.5} = 0.024M^{0.58} \quad (3)$$

with $\langle r_g^2 \rangle^{0.5}$ in nm and M in g/mol. The exponent is the same as that published by Tackx and Tacx.[34]

The radius of gyration of F0 deviates from the linear reference for molar masses above 400 000 g/mol, tending toward smaller

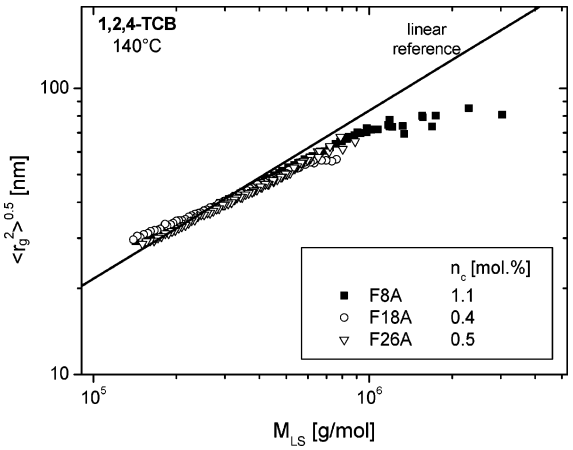

Figure 5. Radius of gyration as a function of molar mass for various copolymers with the lowest comonomer content each.

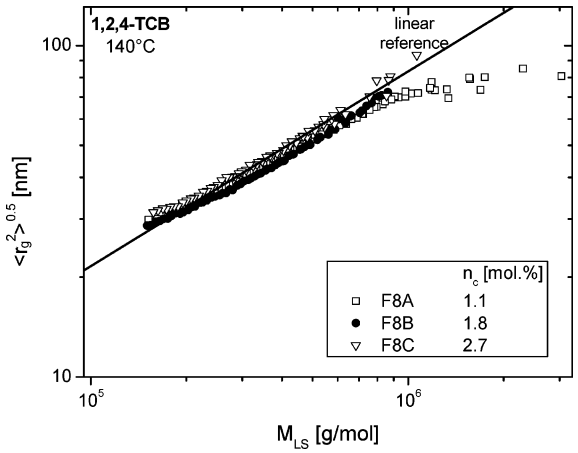

Figure 6. Radius of gyration as a function of molar mass for the octene copolymers.

values, thus indicating a contraction of the coils in solution. Such a contraction is typical of long-chain branched molecules.

Using the Zimm−Stockmayer theory,[35] the average number of three functional branch points per molecule was estimated. If these are assumed to be identical with the number of LCB for F0, a value of 0.3 LCB per molecule can be given, which is in good agreement with the upper limit of 0.37 LCB/molecule determined by NMR.

The influence of comonomer type and concentration on long-chain branching was analyzed based on the comparison of the radii of gyration (cf. Figure 5).

From Figure 5 it can clearly be seen that the radius of gyration of all copolymers with the lowest comonomer contents deviates from the linear reference above molar masses of 400 000 g/mol. (The deviation from the linear behavior at smaller molar masses is mainly due to the physical limitations of the MALLS. At low molar masses the MALLS has a detection limit of about 20 nm due to the wavelength of the laser used.) Thus, it can be concluded that F8A, F18A, and F26A possess long-chain branches. The deviation is smaller than that of the homopolymer F0 (cf. Figure 4). From this finding it can be concluded that these samples are less branched than F0. As the amount of LCB determined for F0 was already small, the amount of LCB in the copolymers is even lower. Hence, a further quantification of LCB in these systems was not undertaken.

Additionally, the decrease of the radius of gyration by short-chain branches also has to be taken into consideration, with significant effects often seen for comonomer contents larger than 20 wt %.[36] However, with the comonomer contents smaller than this value for most copolymers studied, with the exception of F26C, these effects are thought to be small.

To our knowledge, it is the first time that a copolymer with a comonomer longer than octene was investigated by SEC-MALLS. Even the comonomer hexacosene does not decrease the radius of gyration (as found for the linear sample F26C).

For the octene-based copolymers the difference to the linear reference becomes less pronounced with increasing comonomer content, with no deviation seen for F8C (Figure 6). A similar behavior was found for the longer α-olefin copolymers.

From the SEC-MALLS measurements it was concluded that the catalyst system [Ph_2C(2,7-di-*t*-BuFlu)(Cp)]$ZrCl_2$/MAO produced LCB, even if α-olefins of greater than 8 carbons in length were used as comonomers. However, the incorporation of LCB was found only for copolymers containing a low comonomer content. With a maximum LCB content of only 0.61 LCB/10 000 CH_2 determined for F0, the question arises whether the amount of LCB in the samples with a high comonomer content is below the detection threshold for SEC-MALLS or whether long-chain branches are not generated at all. To gain deeper insight into the existence of LCB in these copolymers, rheological measurements were performed, as they are very sensitive with respect to very small amounts of LCB.

Rheological Characterization. Long-chain branching influences a number of linear and nonlinear rheological properties. These include the viscosity function and the dependence of the zero shear rate viscosity (η_0) on the absolute mass-average molar mass M_w. The dependence of the phase angle (δ) on the complex modulus ($|G^*|$) is significantly influenced by the presence of LCB, too.[1] Long-chain branched systems also show increased linear steady-state elastic compliances (J_e^0) if compared with linear counterparts.[26] It should be mentioned, however, that most of these rheological properties are dependent on both LCB and molar mass distribution (MMD). An exception is the relation between η_0 and M_w which was found to be independent of polydispersity within the accuracy of the measurements.[29] All of these rheological properties were used to investigate the presence of LCB in the copolymers as the influence of the molar mass distribution can be neglected due to their similar polydispersity (Table 2).

Zero Shear Rate Viscosity η_0. For the zero shear rate viscosity η_0 the relationship

$$\eta_0 = K_1 M_w^{\alpha} \tag{4}$$

is well established in cases of linear polymers above a critical molar mass M_c, which is about 2 times the entanglement molar mass M_e. At 150 °C the material constants were found to be $K_1 = 9 \times 10^{-15}$ and $\alpha = 3.6$ for linear polyethylenes with η_0 in Pa s and M_w in g/mol. Substantial deviation from this simple relationship occurs with the presence of LCB. For long-chain branched mLLDPE and mHDPE the zero shear rate viscosity was typically found to be greater than the value η_0^{lin}, calculated for a linear sample of the same molar mass using eq 4.[26]

The zero shear rate viscosity η_0 was measured for all samples by means of creep experiments (Figure 1). The results are plotted as a function of M_w in Figure 7. The zero shear rate viscosities of the samples F0, F8A, F18A, F8B, and F18B lie distinctly above the η_0-M_w line established for linear polyethylenes.

The ratio η_0/η_0^{lin} provides a more subtle representation of the influence of the LCB on the zero shear rate viscosities and is very suitable for a discussion of the role of the various comonomers regarding the LCB architecture. Therefore, η_0/η_0^{lin}

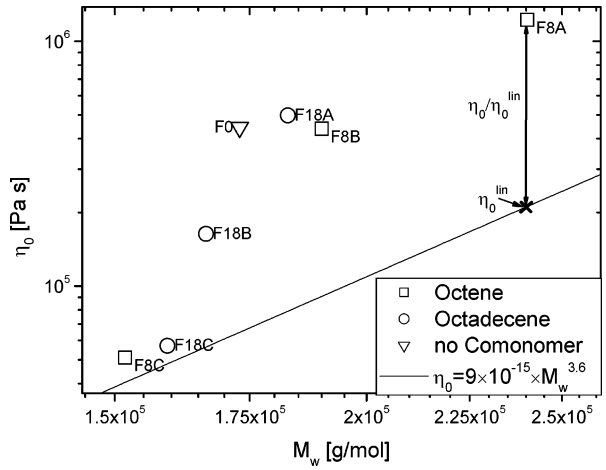

Figure 7. Zero shear rate viscosity η_0 as a function of molar mass M_w for the homopolymer and octene/octadecene copolymers.

is plotted in Figure 8a as a function of the comonomer feed and in Figure 8b in dependence on the comonomer content.

Generally, η_0/η_0^{lin} was found to decrease with increasing feed and comonomer content as well, approaching the ratio of 1 for purely linear systems. The highest increase of the zero shear rate viscosity was observed for F0 with $\eta_0/\eta_0^{lin} \approx 6.9$. The copolymers with the lowest comonomer content (F8A, F18A, and F26A) show an increase of η_0 between 6.3 and 5.5. The copolymers with medium comonomer contents exhibit values of 4.8 and 3.0 for F8B and F18B/F26B, respectively.

The question arises about the nature of the mechanism of the copolymer influencing the LCB formation.

It is evident that each comonomer has a different influence on η_0/η_0^{lin} as a function of feed and content. In general, the incorporation of LCB into the growing chain can be influenced either by the comonomer feed concentration or by the already incorporated comonomer. In the first case the influence is mainly due to diffusion and kinetic effects. It can formally be considered a terpolymerization reaction; ethene, the comonomer, and the LCB-forming macromer act as competing reactants.

For all copolymerizations discussed herein an increase of the polymerization activity was observed up to a certain comonomer concentration in the feed.[23] The activity reached a maximum much higher than that of the ethene homopolymerization and decreased when more than about 10 mol % of comonomer was in the reactor feed. This comonomer effect was observed often in the literature for many metallocene-catalyzed ethene/α-olefin copolymerizations.[37−39] Seppälä et al. ascribe this to a participation of the comonomer on the activation of the active center.[40,41] This leads to a decrease of the activation energy for the insertion of a monomer into the carbon−metal bond and thereby facilitate the chain growth and the chain-transfer reactions. This phenomenon is very catalyst and comonomer specific. For ethene/propene copolymerizations in solution it was furthermore found that the comonomer effect is also lowered with higher ethene concentration in feed.[42] Figure 8a shows for the comomoner feed a decreasing effect on the LCB incorporation with increasing comonomer concentration. Looking at the influence of the reaction mixture there is a less pronounced difference between the comonomer types used; most important is their amount in solution. In contrast to that, the comonomer acts very differently after insertion into the polymer chain. In contrast, after insertion into the polymer chain the various comonomers acted very differently, with the steric hindrance of the polymer side chains strongly determining LCB formation (Figure 8b). For example, although F26C and F8B have approximately the

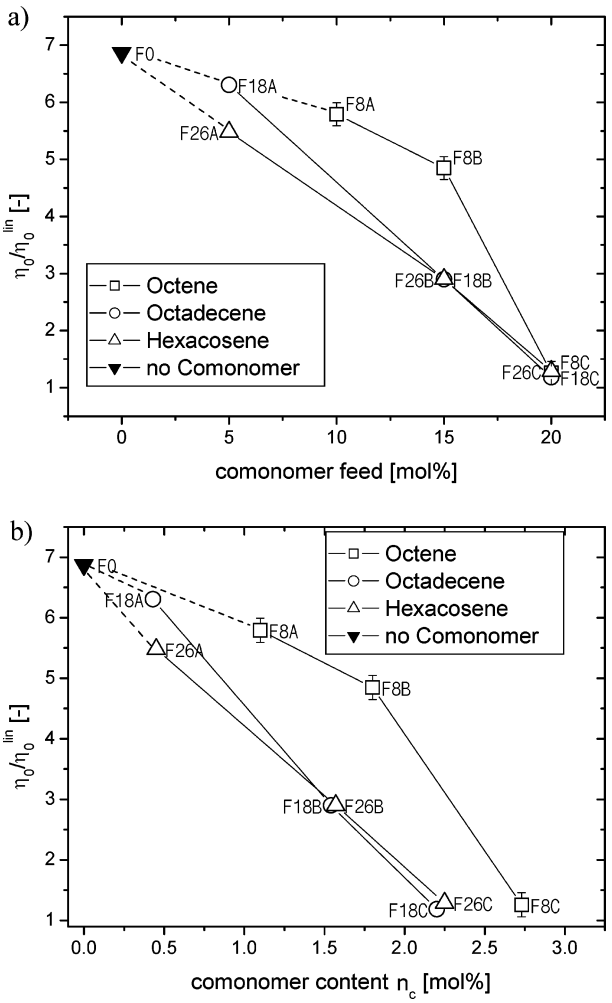

Figure 8. (a, b) Ratio of zero shear rate viscosity η_0/η_0^{lin} as a function of comonomer feed and content, respectively. The approximate experimental error of η_0/η_0^{lin} is about ±20% (shown for the octene series) assuming ±5% error in M_w.

same comonomer content (1.9 mol %), each sample exhibited significantly different viscosity ratios of approximately 5 and 1, respectively. The latter lies on the η_0-M_w line for linear PE (Figure 7). The octadecene (F18) and hexacosene (F26) copolymers did not show a large difference in η_0/η_0^{lin} as a function of the comonomer content n_c. When comparing octadecene and hexacosene copolymers, the comonomer length is not found to play an important role in LCB incorporation. However, comparing octene and octadecene (or hexacosene) polymers, the LCB incorporation is obviously different. Thus, the additional 10 carbons of octadecene have a distinct effect on η_0/η_0^{lin} while the additional 8 carbons between octadecene and hexacosene do not strongly influence this quantity.

As all high comonomer content samples (F8C, F18C, and F26C) are found to lie at $\eta_0/\eta_0^{lin} \approx 1$, it can be concluded that these samples are predominantly linear. This finding is in good agreement with the SEC-MALLS experiments. The effect between the different samples, however, is much more obvious than by SEC-MALLS as the effects are much larger than the small deviations of the radius of gyration of the branched samples from the linear standard.

Viscosity Function. The dynamic viscosities of F18B and F18C are represented over a very wide frequency range in Figure 9. They were obtained by dynamic-mechanical measurements and conversion of creep recovery data.[32] Both samples have the same comonomer and similar molar masses of 167 for F18B

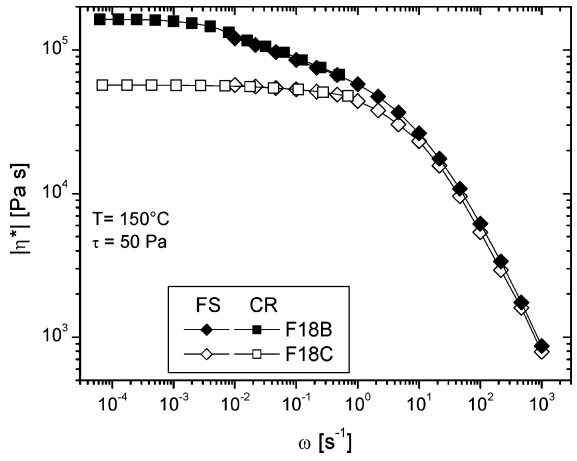

Figure 9. Comparison of the complex viscosities of F18C and F18B obtained by frequency-sweep (FS) and calculated from creep recovery (CR).

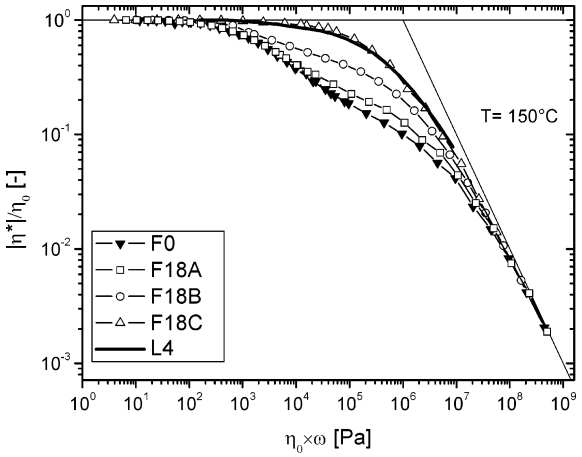

Figure 10. Viscosity functions normalized by η_0 for F0, L4, and the octadecene copolymers.

and 159 kg/mol for F18C, respectively. The dynamic data extracted from the retardation spectrum (calculated from creep recovery tests[32] (an example of a creep recovery test is shown in Figure 1)) overlap very well with the dynamic data from the frequency sweeps.

The viscosity functions of F18B and F18C are distinctly different. Taking molecular parameters into account, this is thought to be a consequence of differing degrees of LCB. At angular frequencies above 10 s^{-1} the viscosity functions $|\eta^*(\omega)|$ of F18B and F18C are similar. However, below this value, F18B exhibits the typical LCB-PE behavior of two distinct "bends" at 10 and 10^{-3} s^{-1}. Only one such "bend" is seen for F18C, being typical of linear samples.

As the two samples differ in zero shear rate viscosity, normalization is needed for further analysis. The normalized viscosity $|\eta^*(\omega)|/\eta_0$ was plotted as a function of the reduced angular frequency $\eta_0\omega$ (Figure 10). This normalization can only be made assuming the validity of the Cox−Merz rule for these samples. However, this has been proven for virtually all single-phase polymer melts. The change in shape of the reduced viscosity functions of F18A, F18B, F18C, F0, and L4 is shown in Figure 10. L4 is a linear ethene/butene copolymer whose rheology can be found in the literature.[26]

At high frequencies a slope of approximately −1 was reached in a double-logarithmic scale. For samples not exhibiting LCB the shape of the viscosity curve depends only on the molar mass distribution. Significant differences are seen for samples containing LCB. From the results in Figure 10 it can be concluded that F18C does not contain a large amount of LCB, which agrees with the findings of SEC-MALLS.

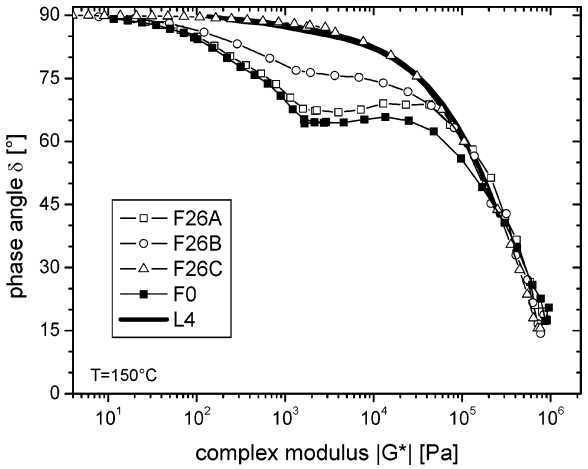

Figure 11. $\delta(|G^*|)$ plot for the samples of the hexacosene series, linear reference (L4), and the homopolymer F0.

While F18C and L4 show no signs of LCB, samples with lower comonomer contents exhibit viscosity functions with a shape typical of LCB which becomes the more pronounced the lower the comonomer content is. F18B shows an intermediate behavior, between that of F18A and F18C.

***|G*|−δ* Plot.** The phase angle δ as a function of the absolute value of the complex modulus $|G^*|$ is another versatile tool for getting insight into the molecular structure, having the advantage that no normalization with respect to the molar mass is needed.

However, a characterization of LCB by the $|G^*|-\delta$ plot is only possible if the shape of the molar mass distribution is known. Bimodal or very broad molar mass distributions show a behavior similar to that of LCB. For all the materials studied having a polydispersity of around 2 these limitations do not apply.

For linear systems the dependence of the phase angle δ with $|G^*|$ is found to sharply increase at small phase angles and approach a plateau upon reaching the limiting phase angle of 90°. A typical linear behavior was seen for F26C (Figure 11); the strongest indication of LCB was observed for F0. The lower comonomer content hexacosene copolymers, F26A and F26B, also show slight deviations from L4 and F26C, suggesting LCB contents between those found in F26C and F0. It can thus be concluded that F0 had the highest degree of LCB followed by F26A and F26B, while F26C showed no indication of LCB. Similar trends with comonomer content were found for the octadecene and hexacosene copolymers.

Steady-State Creep Recovery Compliance J_e^0. The presence of LCB may also be studied using the steady-state creep recovery compliance J_e^0. Since all systems investigated have a similar molar mass distribution and short-chain branching does not effect this property,[26] no dependence on molar mass distribution has to be regarded for the systems investigated here. High molar mass components, which increase J_e^0 significantly,[43] are not observed for any of the copolymers by SEC-MALLS. Thus, the only factor influencing J_e^0 for the materials under investigation is the degree of LCB.

The linear steady-state elastic compliance J_e^0, as a function of the comonomer content n_c, is shown in Figure 12. Because of the long retardation times found for F8A, F18B, and F26B, it was not possible to reach the steady state. For these systems the value of J_e^0 is higher than that measured. The homopolymer

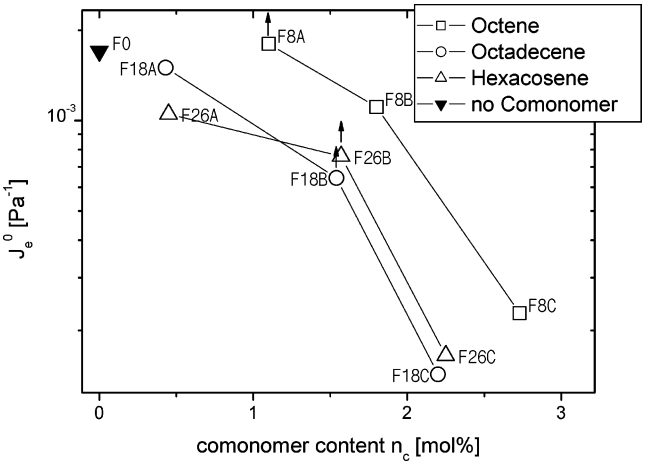

Figure 12. Linear steady-state creep recovery compliance J_e^0 as a function of comonomer. Arrows indicate that the steady state could not be reached.

F0 and the copolymers with a low comonomer content (F8A, F8B, F18A, and F26A) were found to have a value of J_e^0 between 10×10^{-4} and 20×10^{-4} Pa^{-1}. For F18B and F26B slightly lower values of $J_e^0 \approx 7 \times 10^{-4}$ Pa^{-1} were observed. These data are all within the typical range previously reported for narrowly distributed LCB-mPE.[26] For the higher comonomer content copolymers (F8C, F18C, and F26C) J_e^0 is slightly above 10^{-4} Pa^{-1}, which indicates an absence of LCB.[26]

Conclusions

For the homopolymer, a maximum degree of long-chain branching of 0.37 and 0.30 LCB/molecule was determined by melt-state NMR and SEC-MALLS, respectively. Good agreement is seen considering the small contents quantified, both of which being at the lower limit of detection for the two techniques, and the simplifying assumptions of the Zimm−Stockmayer theory.[35] For the copolymers, smaller LCB contents were found with SEC-MALLS. The resolution of this classical method is not high enough, however, for a clear discrimination of the influence of the various comonomers on the LCB content.

Therefore, rheology was used to further distinguish between the LCB content as some rheological quantities have been proven to react very sensitively on the existence of long-chain branches. Lower degrees of LCB were detected in the copolymers than were found in the homopolymer. Higher comonomer content and comonomers of greater length were also found to result in lower degrees of LCB, in qualitative agreement with the SEC-MALLS measurements. Because of the high sensitivity of rheological methods with respect to LCB, a clearer discrimination could be gained from the results.

The results of the SEC-MALLS and more pronounced the rheological characterization indicate for this series of copolymers that the catalyst used produced linear and long-chain branched samples depending on the comonomer content. The homopolymer showed the highest long-chain branch content. Any addition of comonomer decreased the degree of long-chain branching. For the samples with the highest comonomer content no long-chain branches were detected neither by SEC-MALLS nor by rheology. This effect depends on both the molar mass (length) and the content of the comonomer. The LCB content decreases with growing number of incorporated comonomers per chain and with their increase in length. For the samples with the lowest comonomer content only a very small difference to the homopolymer was found. Similar results are reported by Kokko et al.[19] and Walter et al.,[44] but in these articles only one comonomer was used. The dependency of the long-chain branch incorporation and thus of the rheological properties on the comonomer feed was also investigated for different catalyst systems by the groups of Mülhaupt[44] and Seppälä.[18,19,24,25] The long-chain branch incorporation ceases at much higher comonomer contents, however, than shown in this study. These differences can be related to the use of hydrogen gas for molar mass control and the different catalyst systems in this study.

While a clear difference in LCB content was observed between the polymers copolymerized with octene and octadecene, the difference between those with hexacosene and octadecene is small. These findings can be understood when looking at the chemical mechanism of the long-chain branch incorporation. A short-chain branch of longer length provides a stronger steric hindrance concerning the incorporation of a vinyl-terminated macromonomer into the growing chain than that of a smaller length. The effectiveness of octadecene and hexacosene seems to be above a steric threshold, where the hindrance is so strong that macromers are not attached to the backbone anymore. These conclusions could only be attained by using hexacosene as comonomer which has not been previously investigated in the literature for the metallocene-catalyzed synthesis of polyethylenes.

Acknowledgment. The authors gratefully acknowledge the financial support of Deutsche Forschungsgemeinschaft (DFG) and thank the following persons for their contributions: Mrs. Inge Herzer (LSP) for SEC-MALLS measurements, Jens Stange (LSP) for valuable discussions, Manfred Hehn and Hans-Peter Reich (MPIP) for their assistance with NMR-hardware-related issues, and Prof. Dr. Hans-Wolfgang Spiess (MPIP) for his continuous support. M. Parkinson acknowledges the financial support from Total S.A.

References and Notes

(1) Piel, C.; Stadler, F. J.; Kaschta, J.; Rulhoff, S.; Münstedt, H.; Kaminsky, W. Structure−Property Relationships of Linear and Long-Chain Branched Metallocene High Density Polyethylenes Characterized by Shear Rheology and SEC-MALLS. *Macromol. Chem. Phys.* **2006**, *206*(1), 26−38.
(2) Mülhaupt, R. *Macromol. Chem. Phys.* **2003**, *204*, 289−327.
(3) Böhm, L. L. *Angew. Chem., Int. Ed.* **2003**, *42*, 5010−5030.
(4) Resconi, L.; Cavallo, L.; Fait, A.; Piemontesi, F. *Chem. Rev.* **2000**, *100*, 1253−1345.
(5) Heuer, B.; Kaminsky, W. *Macromolecules* **2005**, *38*, 3054−3059.
(6) Coates, G. W. *Polymer* **2000**, *100*, 1223−1252.
(7) Sperber, O.; Kaminsky, W. *Macromolecules* **2003**, *36*, 9014−9019.
(8) Koivumäki, J.; Fink, G.; Seppälä, J. V. *Macromolecules* **1994**, *27*, 6254−6258.
(9) Hoff, M.; Kaminsky, W. *Macromol. Chem. Phys.* **2004**, *205*, 1167−1173.
(10) Lai, S. Y.; Wilson, J. R.; Knight, G. W.; Stevens, J. C.; Chum, P. W. S. Elastic substantially linear olefin polymers. 5,272,236, 1993.
(11) Brant, P.; Canich, J. A. M.; Dias, A. J.; Bamberger, R. L.; Licciardi, G. F.; Henrichs, P. M. Long-chain branched polymers and a process to make long-chain branched polymers. WO 94/07930, 1994.
(12) Woo, T. K.; Margl, P. M.; Ziegler, T.; Blochl, P. E. *Organometallics* **1997**, *16*, 3454−3468.
(13) Harrison, D.; Coulter, I. M.; Wang, S. T.; Nistala, S.; Kuntz, B. A.; Pigeon, M.; Tian, J.; Collins, S. *J. Mol. Catal. A: Chem.* **1998**, *128*, 65−77.
(14) Malmberg, A.; Kokko, E.; Lehmus, P.; Löfgren, B.; Seppälä, J. *Macromolecules* **1998**, *31*, 8448−8454.
(15) Wood-Adams, P. M.; Dealy, J. M.; deGroot, A. W.; Redwine, O. D. *Macromolecules* **2000**, *33*, 7489−7499.
(16) Beigzadeh, D.; Soares, J. B. P.; Hamielec, A. E. *J. Appl. Polym. Sci.* **1999**, *71*, 1753−1770.
(17) Gabriel, C.; Kokko, E.; Löfgren, B.; Seppälä, J.; Münstedt, H. *Polymer* **2002**, *43*, 6383−6390.

(18) Kokko, E.; Lehmus, P.; Malmberg, A.; Löfgren, B.; Seppälä, J. V. *Long-Chain Branched Polyethene via Metallocene-Catalysis: Comparison of Catalysts*; Springer: Berlin, 2001; pp 335−345.
(19) Kokko, E.; Malmberg, A.; Lehmus, P.; Löfgren, B.; Seppälä, J. V. *J. Polym. Sci., Part A: Polym. Chem.* **2000**, *38*, 376−388.
(20) Kolodka, E.; Wang, W.-J.; Charpentier, P. A.; Zhu, S.; Hamielec, A. E. *Polymer* **2000**, *41*, 3985−3991.
(21) Wang, W. J.; Yan, D. J.; Zhu, S. P.; Hamielec, A. E. *Macromolecules* **1998**, *31*, 8677−8683.
(22) Soga, K.; Uozumi, T.; Nakamura, S.; Toneri, T.; Teranishi, T.; Sano, T.; Arai, T.; Shiono, T. *Macromol. Chem. Phys.* **1996**, *197*, 4237−4251.
(23) Kaminsky, W.; Piel, C.; Scharlach, K. *Macromol. Symp.* **2005**, *226*, 25−34.
(24) Kokko, E.; Pietikäinen, P.; Koivunen, J.; Seppälä, J. V. *J. Polym. Sci., Part A: Polym. Chem.* **2001**, *39*, 3805−3817.
(25) Lehmus, P.; Kokko, E.; Harkki, O.; Leino, R.; Luttikhedde, H.; Nasman, J.; Seppälä, J. *Macromolecules* **1999**, *32*, 3547−3552.
(26) Gabriel, C.; Münstedt, H. *Rheol. Acta* **2002**, *41*, 232−244.
(27) Münstedt, H.; Steffl, T.; Malmberg, A. *Rheol. Acta* **2005**, *45*, 14−22.
(28) Piel, C.; Starck, P.; Seppälä, J. V.; Kaminsky, W. Thermal and Mechanical Analysis of Metallocene-Catalyzed Ethylene-α-Olefin Copolymers: The influence of length and number of the crystallizing side-chains. *J. Polym. Sci., Part A: Polym. Chem.*, in press.
(29) Stadler, F. J.; Piel, C.; Kaschta, J.; Rulhoff, S.; Kaminsky, W.; Münstedt, H. Dependence of the zero shear-rate viscosity and the viscosity function of linear high density polyethylenes on the mass-average molar mass and polydispersity. *Rheol. Acta*, in press.
(30) Klimke, K.; Parkinson, M.; Piel, C.; Kaminsky, W.; Spiess, H.-W.; Wilhelm, M. Optimized Polyolefin Branch Quantification by Melt-State ^{13}C NMR Spectroscopy. *Macromol. Chem. Phys.*, in press.
(31) Gabriel, C.; Kaschta, J. *Rheol. Acta* **1998**, *37*, 358−364.
(32) Kaschta, J.; Schwarzl, F. R. *Rheol. Acta* **1994**, *33*, 517−529.
(33) Wood-Adams, P.; Costeux, S. *Macromolecules* **2001**, *34*, 6281−6290.
(34) Tackx, P.; Tacx, J. C. J. F. *Polymer* **1998**, *39*, 3109−3113.
(35) Zimm, B. H. M.; Stockmayer, W. H. *J. Chem. Phys.* **1949**, *17*, 1301−1314.
(36) Sun, T.; Brant, P.; Chance, R. R.; Graessley, W. W. *Macromolecules* **2001**, *34*, 6812−6820.
(37) Kaminsky, W. *J. Polym. Sci., Part A: Polym. Chem.* **2004**, *42*, 3911−3921.
(38) Quijada, R.; Dupont, J.; Miranda, M. S. L.; Scipioni, R. B.; Galland, G. B. *Macromol. Chem. Phys.* **1995**, *196*, 3991−4000.
(39) Chien, J. C. W.; Nozaki, T. *J. Polym. Sci., Part A: Polym. Chem.* **1993**, *31*, 227−237.
(40) Seppälä, J. V.; Koivumäki, J.; Liu, X. *J. Polym. Sci., Part A: Polym. Chem.* **1993**, *31*, 3447−3452.
(41) Koivumäki, J.; Seppälä, J. V. *Macromolecules* **1993**, *26*, 5535−5538.
(42) Villar, M. A.; Ferreira, M. L. *J. Polym. Sci., Part A: Polym. Chem.* **2001**, *39*, 1136−1148.
(43) Münstedt, H. Polymerschmelzen. In *Fliessverhalten von stoffen und stoffgemischen*; Kulicke, W., Ed. Hüthig&Wepf-Verlag: Basel, 1986; pp 238−279.
(44) Walter, P.; Trinkle, S.; Suhm, J.; Mäder, D.; Friedrich, C.; Mülhaupt, R. *Macromol. Chem. Phys.* **2000**, *201*, 604−612.

MA0514018